Performance of Impedance Transformer for High-Power ICRF Heating in LHD

Kenji Saito[1], Testuo Seki[1], Hiroshi Kasahara[1], Ryosuke Seki[1], Shuji Kamio[1], Goro Nomura[1] and Takashi Mutoh[1]

[1]National Institute for Fusion Science, National Institutes of Natural Sciences, Toki, Gifu 509-5292, Japan

E-mail: saito@nifs.ac.jp

Abstract. There are two types of ion cyclotron range of frequencies antennas in the Large Helical Device. The handshake form (HAS) antenna has high heating efficiency. However, its loading resistance is small, and injection power is limited by the voltage of the transmission line. On the other hand, the field-aligned-impedance-transforming (FAIT) antenna has higher loading resistance than the HAS antenna despite having a smaller antenna head. However, the high voltage on the transmission line is again the bottleneck for high-power injection, as with the HAS antenna. We developed an ex-vessel impedance transformer for the HAS and FAIT antennas to decrease the voltage on the transmission lines by increasing loading resistance. The estimated enhancement factors of loading resistance were 1.65 and 2.50 for the HAS and the FAIT antennas, respectively, and the experimental result for the HAS antenna was consistent with the estimation. Therefore, higher power injection will be possible.

1. Introduction

In the Large Helical Device (LHD) [1], there are presently two pairs of ion cyclotron range of frequencies (ICRF) antennas. They are referred to as the handshake form (HAS) antennas [2] and the field-aligned-impedance-transforming (FAIT) antennas [3]. The heads of the HAS antennas are aligned in the direction of the magnetic field lines to excite waves with a large wavenumber component parallel to the magnetic field lines. Therefore, the HAS antenna has high performance in heating efficiency of minority ion heating at the 0-π current phase [4], where heating efficiency is defined as the power absorbed by plasma divided by the injected power from the antenna. However, the loading resistance R, defined by $R = 2P\ (z_c/V_{max})^2 = z_c/VSWR$, was small, and the maximum injection power was limited by the voltage on the transmission line, where P is the forward power minus the reflected power, and V_{max} is the maximum voltage on the line with the characteristic impedance z_c, which is 50 Ω in the LHD. In this paper, loading resistance is defined on the transmission line not on the antenna head, and it is equivalent to the impedance at the voltage node on the transmission line. We limit the V_{max} to 30 kV in normal operation to prevent breakdowns on the transmission line, and the interlock level of V_{max} is normally set to 35 kV. The power feedback system [5] decreases the injection power if the voltage is increased beyond 30 kV, and the interlock system turns off the power immediately if the voltage reaches 35 kV. The typical plasma loading resistance R_p of the HAS antenna was only 2 Ω, where the loading resistance of vacuum injection was subtracted to eliminate loading resistance caused by the circuit loss. The maximum injection power calculated with the plasma loading resistance of 2 Ω and the voltage limit of 30 kV is only 360 kW.

The heads of the FAIT antennas are aligned in the direction perpendicular to the magnetic field lines; however, heating efficiency is comparable to that of the HAS antennas [6]. Meanwhile, although the area of the Faraday-shield of the FAIT antenna is approximately half of that of the HAS antenna, it has a higher plasma loading resistance of typically 5 Ω due to the optimized in-vessel impedance transformer between the antenna head and the ceramic feed-through [3,7]. It was deduced from the equation $P = \frac{1}{2} R\,(V_{max}/z_c)^2$ that an injection power of 1.8 MW or power density (injection power normalized by the area of Faraday-shield) of 15 MW/m^2 would be possible for several seconds. This was because a voltage of 38.5 kV was once applied as a trial on the transmission line without arcing on the antenna head, and the plasma loading resistance $R_p > 6\ \Omega$ was realized with a line-averaged electron density of more than $2 \times 10^{19}\ m^{-3}$ at the standard antenna position [3]. However, application of voltage of 38.5 kV on the transmission line may cause breakdowns on the transmission line. Once a breakdown occurs in the transmission line, high voltage cannot be applied to the transmission line again. Therefore, to reduce the voltage without decreasing the injection power, we developed an ex-vessel impedance transformer (EVIT).

In section 2, we present the detailed design of the EVIT. An electromagnetic simulation of the designed EVIT is conducted in section 3, and section 4 demonstrates its high performance experimentally. Section 5 presents the summary.

2. Design of ex-vessel impedance transformer

In order to decrease the maximum voltage on the transmission line by increasing the loading resistance, conversion of impedance near the antenna port is necessary. A pre-stub tuner was one of the candidates, however, space is limited around the antenna port. Moreover, the in-vessel impedance transformer for the FAIT antenna worked well [3]. Therefore, we decided to develop a compact ex-vessel impedance transformer (EVIT) for the HAS and FAIT antennas inserted in the transmission line outside the vacuum vessel at the port of the ceramic feed-through. The drawback of the impedance transformer is that the frequency is fixed. The frequency for the EVIT was set to 38.5 MHz, which is the design frequency for the FAIT antennas, since this frequency is favourable for minority ion heating at the standard magnetic field of 2.75 T on the magnetic axis at the major radius of 3.6 m [8,9]. This frequency is also favourable for the second-harmonic heating of deuterium plasma.

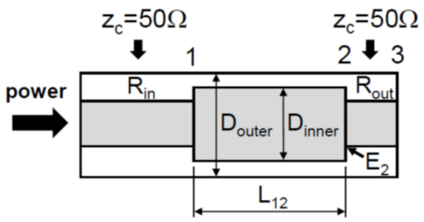

Figure 1. Simple model of the EVIT. D_{outer} is the diameter of the outer conductor; D_{inner} and L_{12} are the diameter and length of the inner conductor between points 1 and 2, respectively. R_{in} is the converted loading resistance on the transmission line on the input side with the characteristic impedance of 50 Ω, and R_{out} is the loading resistance between points 2 and 3, where the characteristic impedance is also 50 Ω.

In order to determine the dimensions of the EVIT, simulations were conducted with the simple model shown in figure 1, where the length and diameter of the inner conductor between points 1 and 2 were variable. The diameter of the outer conductor was ϕ 241 mm, which is the same as that of the transmission line. The direction of the electric field was assumed to be radial. Point 3 is the port of the ceramic feed-through, and a bellows is inserted between points 2 and 3 in order to absorb the deformation of the ceramic feed-through. Therefore, a 100 mm length is necessary between points 2 and 3. The following equation was used for the rough estimation of the electric field E:

$$E = \frac{V}{r \ln(D_{outer} / D_{inner})} \tag{1}$$

where V is the voltage applied on the inner conductor, r is the distance from the axis, and D_{outer} and D_{inner} are the diameters of the outer and inner conductors, respectively. The value of impedance at point 2 must be obtained in order to calculate the converted loading resistance and the maximum strength of the electric field in the impedance transformer.

The length L is defined as the distance between a voltage node in the transmission line and the impedance matching device, including the uncertainty of a half wavelength multiplied by an integer. The loading resistance R corresponds to the impedance at the node. For the upper and lower port FAIT antennas, the maps of plasma loading resistance R_p (= R-R_{vacuum}) and the shift of voltage node ΔL (= L-L_{vacuum}) were obtained before the installation of the EVIT, as shown in figures 2(a) and (b), where the subscript 'vacuum' means injection to the vacuum without plasma. The typical values of R = 5.6 Ω (R_p = 5 Ω, R_{vacuum} = 0.6 Ω) and L = L_{vacuum}-0.05 m shown by '+' were used for the design of the EVIT. For the HAS antenna, R = 2.3 Ω (R_p = 2 Ω, R_{vacuum} = 0.3 Ω) was used as the typical loading resistance. Data of ΔL for the HAS antennas is insufficient. Therefore, we assumed L = L_{vacuum} as the typical value. The typical impedances at point 2 for the FAIT and HAS antennas were calculated from the values of R and L as 6.6+21.3j Ω and 4.7+50.7j Ω, respectively. Whereas the differences in impedance between upper and lower port antennas were small, therefore, they were averaged.

Figure 3(a) shows the enhancement factor of loading resistance R_{in}/R_{out} for the FAIT antenna calculated with the obtained typical impedance. The high-enhancement factor

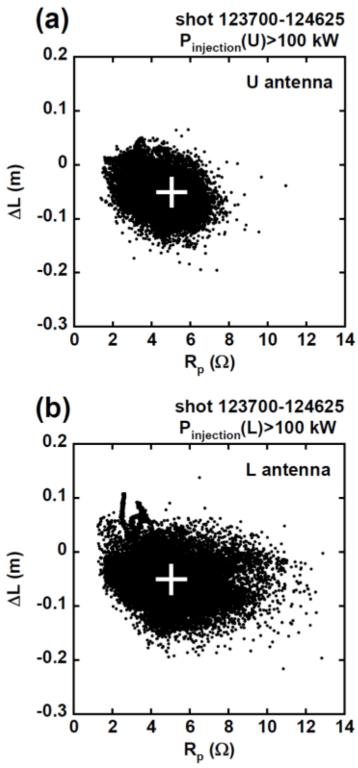

Figure 2. R_p-ΔL maps for (a) upper and (b) lower port FAIT antennas.

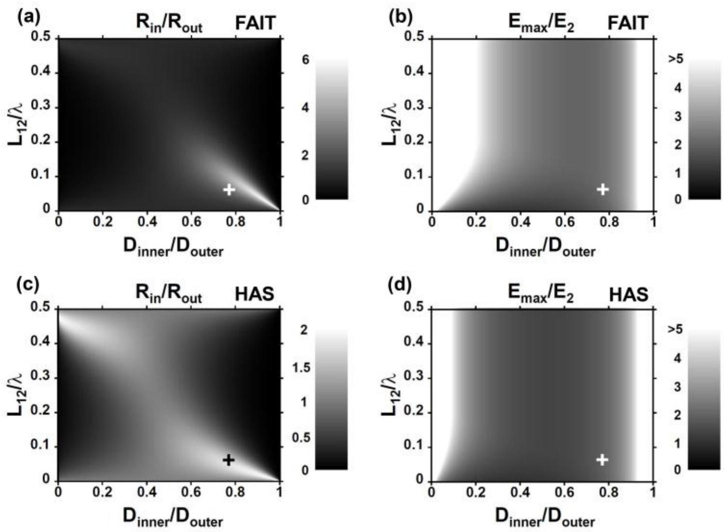

Figure 3. Contours of enhancement factor R_{in}/R_{out} and the normalized maximum strength of the electric field E_{max}/E_2. The ordinate is the length of the inner conductor normalized by the wavelength λ, and the abscissa is the ratio of the diameters of the inner and outer conductors. (a) R_{in}/R_{out} for the FAIT antenna; (b) E_{max}/E_2 for the FAIT antenna; (c) R_{in}/R_{out} for the HAS antenna; (d) E_{max}/E_2 for the HAS antenna.

region was located in the short L_{12} and large D_{inner}. The short L_{12} was favourable for the design of a compact EVIT. Figure 3(b) shows the maximum electric field normalized by E_2 shown in figure 1. We determined L_{12} = 495 mm and D_{inner} = ϕ 186 mm as shown by the '+', since the value of L_{12} was the maximum for the limited space, and the larger D_{inner} increased the electric field, although the larger L_{12} and D_{inner} increased loading resistance. At the design values of L_{12} and D_{inner}, the enhancement factor was 2.82, and the normalized maximum electric field was 2.13. They were also calculated for the HAS antenna with scanning L_{12} and D_{inner}, as shown in figures 3(c) and (d). In this case, two regions of high-enhancement factor appeared, and it was determined that the design values of L_{12} = 495 mm and D_{inner} = ϕ186 mm for the FAIT antenna were also useful for the HAS antenna, where the enhancement factor and the normalized maximum electric field were 1.64 and 1.88, respectively.

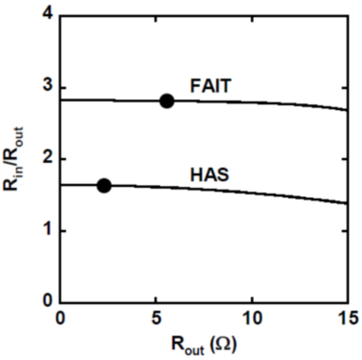

Figure 4. Dependency of enhancement factor on the loading resistance in the output side of EVIT. Closed circles denote the typical discharge.

From the model calculations, we also found that the dependency of the enhancement factor on the loading resistance R_{out} at the output port was weak, as shown in figure 4, where the position of the voltage node in the antenna side was fixed. Therefore, the difference in enhancement factor between the FAIT and HAS antennas was mainly caused by the position of the voltage node. With a characteristic impedance z_{ct} of 15.7 Ω calculated from the diameters of inner and outer conductors between points 1 and 2, the reflection coefficient Γ on the transmission line with a characteristic impedance of z_c was calculated by changing the position of point 1, and plotted on Smith charts, as shown in figures 5(a) and (b). The equation of the locus is given as follows:

$$\frac{|\Gamma + (z_c - z_{ct})/(z_c + z_{ct})|}{|\Gamma + (z_c + z_{ct})/(z_c - z_{ct})|} = \frac{|\Gamma + 0.52|}{|\Gamma + 1.92|} = \text{const.} \quad (2)$$

This equation describes the circle of Apollonius for which the center is on Im(Γ)=0. The center of the locus is located in the negative Re(Γ) region, therefore, |Γ| decreases and as a consequence, loading resistance increases. With the obtained values of L_{12} and D_{inner}, we designed the compact EVIT. Figure 6 shows the upper port FAIT antenna with the EVIT. The outer conductor of the EVIT was made with aluminum and the inner conductor was coated with silver on stainless steel to reduce power loss. The flange-to-flange length was only 628 mm, and the edge of the

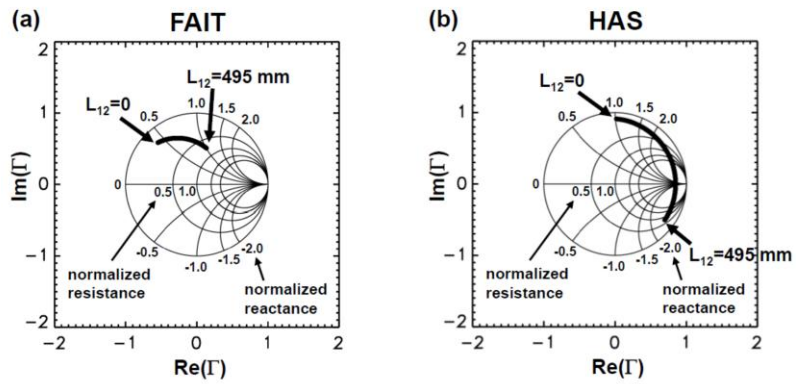

Figure 5. The locus of reflection coefficient on Smith charts for (a) FAIT and (b) HAS antennas.

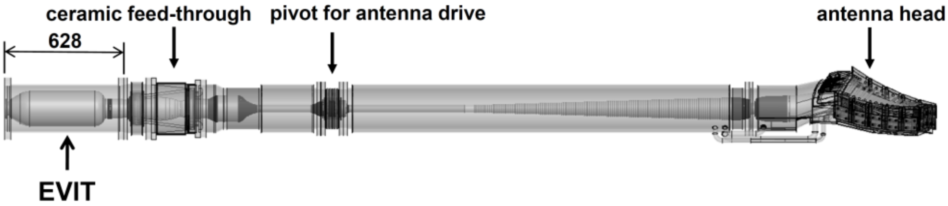

Figure 6. The upper port FAIT antenna with the EVIT.

thick inner conductor was rounded in order to avoid the convergence of electric field lines.

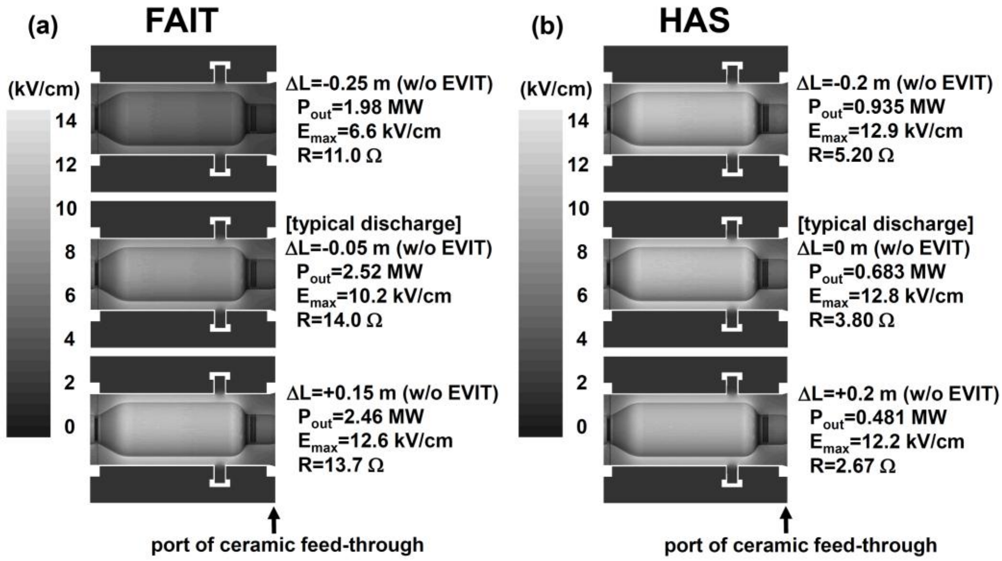

Figure 7. The strength of the electric field in the EVIT for (a) FAIT and (b) HAS antennas depending on the voltage node position ΔL without the EVIT. The maximum voltage in the transmission line was set to 30 kV. The output power P_{out}, the maximum electric field strength E_{max}, and the loading resistances R with the EVIT are also shown. The loading resistances of the FAIT and HAS antennas without the EVIT are 5.6 Ω and 2.3 Ω, respectively.

3. Electromagnetic simulation of ex-vessel impedance transformer

Electromagnetic simulation was performed with HFSS, as shown in figures 7(a) and (b), to obtain detailed estimation of the enhanced loading resistance and the strength of the electric field. The frequency was 38.5 MHz and the maximum voltage in the transmission line connected to the EVIT was set to the operational limit of 30 kV by adjusting output power. The estimated enhancement factor of loading resistance was 2.50 and 1.65 for FAIT and HAS antennas, respectively, at the typical discharge. These were consistent with the calculations by the simple model shown in figure 1. We also changed the voltage node position on the antenna side by ±20 cm, for the enhancement factor strongly depends on this position, as mentioned in section 2. The range of ±20 cm was enough for the FAIT antennas according to figures 2(a) and (b), although data for the HAS antennas was insufficient. In the case of the FAIT

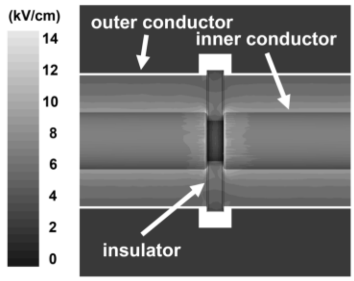

Figure 8. The strength of the electric field near the insulator. The applied voltage was 35 kV.

antenna, the loading resistance was kept high. On the other hand, in the case of the HAS antenna, the enhancement factor was small when the voltage node shifted to the antenna side by 20 cm, but still larger than unity ($R_{in}/R_{out} = 1.16$). The power loss in the transmission line was approximately inversely proportional to the loading resistance. Therefore, the power loss decreased to 40% and 60% for the FAIT and HAS antennas, respectively, in the typical discharge.

The electric field in the transmission line around the PTFE (polytetrafluoroethylene) insulator for the support of the inner conductor was also simulated in order to investigate the breakdown condition as shown in figure 8. The frequency was 38.5MHz and the applied voltage was 35 kV, which is the interlock level, and breakdowns sometimes occurred at the insulator beyond this voltage, although nitrogen was filled at a pressure of 0.3 MPaG in order to prevent breakdowns. The simulated maximum electric field was 13.5 kV/cm at the edge of the inner conductor. As shown in figures 7(a) and (b), the maximum strength of the electric field in the EVITs, where nitrogen is also filled at the pressure of 0.3 MPaG, is smaller than 13.5 kV/cm in all cases in the figures. Therefore, breakdowns in EVITs will be avoided if the voltage in the transmission line is limited to 30 kV.

4. Enhancement of loading resistance in the HAS antenna

EVITs were attached to the HAS antennas in 2014. We measured the reflection coefficient of the HAS antenna at the lower port without plasma using a network analyser, and compared the reflection coefficient to that before the installation of EVIT. At a frequency of 38.5 MHz, the loading resistance without plasma R_{vacuum} was 0.296 Ω before installing the EVIT, and it increased to 0.537 Ω after the installation. The enhancement factor in vacuum injection was 1.81, which almost agreed with the simulated result of 1.71 by HFSS. The voltage node position on the transmission line L_{vacuum} was shifted to the antenna side by 0.764 m, which also agreed well with the simulated result of 0.752 m. At the frequency of 77 MHz, which corresponds to the frequency of the second-harmonic heating of hydrogen, the loading resistance decreased from 0.441 to 0.213 Ω. Therefore, in the HAS antenna, the EVIT was not suitable for this frequency.

In the plasma experiments with the frequency of 38.5 MHz, loading resistance with and without the EVIT for the lower HAS antenna was compared changing the distance Δ between the Faraday-shield and the last closed flux surface, as shown in figure 9. The upper port antenna was turned off in order to avoid the mutual coupling effect. The range in line-averaged electron density was from 0.8 to 1.5 × 10^{19} m^{-3}, and the major radius of the magnetic axis and strength of the magnetic field on the axis were 3.6 m and 2.75 T, respectively, in both experiments. As a reference, data from the lower port FAIT antenna were plotted. These data showed that the conditions were nearly the same in both experiments, since the EVIT was not attached in the FAIT antenna in both experiments. The loading resistance of the HAS antenna was approximately doubled by the EVIT. The shift of voltage node ΔL for the HAS antenna was negligible in both experiments. In this case, the simulated enhancement factor was 1.65, which was consistent with the experiments. Higher power injection was enabled by the enhancement of loading resistance in the HAS antennas.

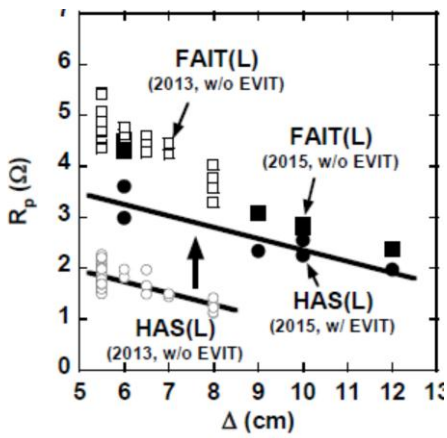

Figure 9. Comparison of R_p with and without EVIT in various antenna positions.

5. Summary

Compact EVITs were developed and installed in the ICRF antennas in the LHD to increase loading resistance in order to increase the ICRF injection power. This was because high voltage on the transmission line had been the bottleneck in high-power operation. High loading resistance is also favourable for the reduction of power loss in the transmission line. Plasma experiments were conducted with and without the EVIT using a HAS antenna. In the experiments, the loading resistance increased, and the experimental enhancement factor of approximately 2 was consistent with that obtained by the simulation (1.65). According to the simulation, the EVIT will also increase the loading resistance of the FAIT antennas by 2.5 times in the typical discharge and as a consequence, a high-power injection of 1.8 MW from one FAIT antenna will be possible.

Acknowledgement

The authors would like to thank the staff of the LHD Experiment Group at the National Institute for Fusion Science for their helpful support during this work. This work was supported by NIFS budget ULRR703.

References

[1] Kaneko O, Yamada H, Inagaki S, Jakubowski M, Kajita S, Kitajima S, et al., 2013 *Nucl. Fusion* **53** 104015.
[2] Kasahara H, Seki T, Saito K, Kumazawa R, Mutoh T, Shimpo F, et al., 2010 *Plasma and Fusion Research* **5** S2090.
[3] Saito K, Seki T, Kasahara H, Seki R, Kamio S, Nomura G, et al., 2015 *Fusion Eng. Des.* **96-97** 583-588.
[4] Kasahara H, Saito K, Seki T, Kumazawa R, Nomura G, Shimpo F, et al., 2011 *Proc. 38th EPS Conf. Strasbourg* P2.099 and http://ocs.ciemat.es/EPS2011PAP/pdf/P2.099.pdf.
[5] Kamio S, Kasahara H, Seki T, Saito K, Seki R, Nomura G, et al., 2015 *Fusion Eng. Des.* **101** 226-230.
[6] Kamio S, Seki T, Saito K, Kasahara H, Seki R, Nomura G, et al., 2015 *Proc. 42nd EPS Conf. Lisbon* P5.154 and http://ocs.ciemat.es/EPS2015PAP/pdf/P5.154.pdf.
[7] Saito K, Seki T, Kasahara H, Seki R, Kumazawa R, Nomura G, et al., 2013 *Fusion Eng. Des.* **88** 1025-1029.
[8] Saito K, Kumazawa R, Mutoh T, Seki T, Watari T, Torii Y, et al., 2001 *Nucl. Fusion* **41** 1021-1035.
[9] Saito K, Kumazawa R, Seki T, Kasahara H, Osakabe M, Isobe M, et al., 2010 *Fusion Science and Technology* **58** 515-523.